

Analysis of Spiral Resonator Filters

Improved performance coupled with reduced size requires the development of novel filter designs for use in advanced wireless systems.

BY SERGEI P. YUSHANOV, JEFFREY S. CROMPTON, AND KYLE C. KOPPENHOEFER, ALTASIM TECHNOLOGIES

Increasing demand for more advanced wireless systems necessitates the introduction of novel designs that are capable of simultaneously fulfilling multiple operating and performance criteria. The implementation of high data rate transmission systems has required the development of innovative designs for microwave filters that must fit within a reduced volume to allow integration of multiple filters in more compact wireless systems. Additionally, the filter's specific passband frequencies and quality factors must be achieved within the system's geometrical and topological constraints. Spiral resonator filters offer one option for significantly reduced size compared to conventional ring resonators. An array of spiral resonators can be directly fabricated on a printed circuit board and because of their characteristic response, they can be designed to occupy minimal volume.

To characterize the operation of these devices, a mathematical construct named the scattering matrix (S -matrix) is used that describes how the RF signal interacts with the device. The signal may reflect, exit other ports and dissipate via heat or electromagnetic radiation; the S -matrix represents each of these signal paths. The order of this matrix is $n \times n$ with n equaling the number of ports in the system; thus, S_{ij} represents the scattering for the j input port and the i output port such that S_{11} specifies

the ratio of signal reflected from port 1 for an input on port 1, and S_{21} specifies the response at port 2 due to a signal at port 1.

Spiral Resonator Simulation

A compact microstrip filter (see Figure 1) using spiral resonators was designed to produce a resonant frequency of 7.2 GHz (Lim *et al.*)

A model was set up using COMSOL Multiphysics (see Figure 2), in which the microstrip line is represented as a perfect electric conductor (PEC) surface on a dielectric substrate, with another PEC surface on the bottom of this substrate

acting as a ground plane. Two lumped ports are modeled as small rectangular faces that bridge the gap between the PEC faces of the ground plane and the microstrip line at each port. A small air domain bounded by a scattering boundary (SBC) surface is added to avoid back reflection of radiated fields and reduce the size of the modeling domain. The model includes the dielectric substrate defined as a volume with the relative permittivity of the dielectric.

The experimental and simulation results for and over a range of frequencies of interest are shown in Figure 3, where S_{11} specifies the ratio of signal reflected from

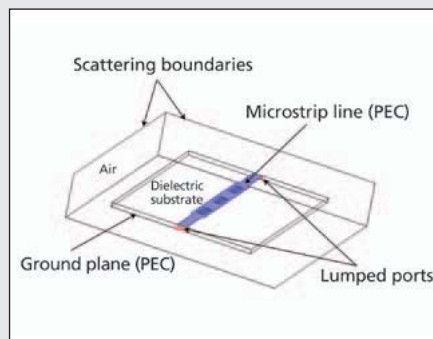


FIGURE 2: Model of the bandstop resonator filter. Some exterior faces are removed for visualization.

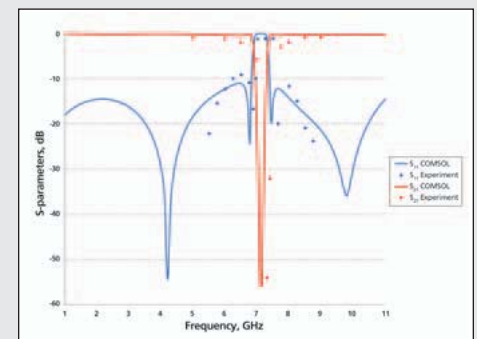


FIGURE 3: Frequency response of the bandstop spiral resonator filter comparing experimental measurement (Lim *et al.*) with COMSOL simulation.

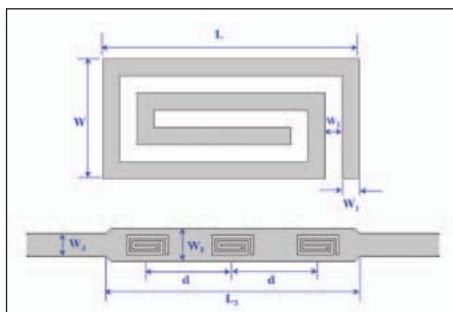


FIGURE 1: Microstrip filter based on rectangular type spiral resonators etched on the center line of the microstrip.

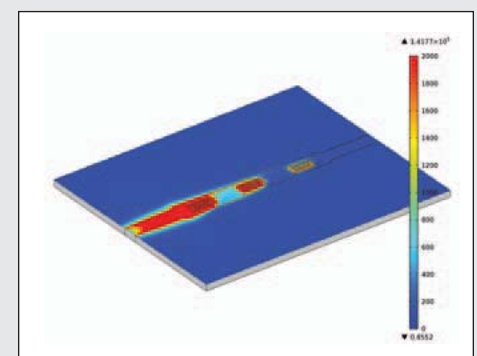
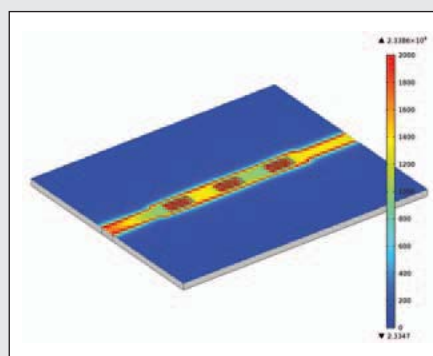


FIGURE 4: Electric field (left) and at (right) resonant frequency.

port 1 for an input on port 1, while S_{21} specifies the response at port 2 due to a signal at port 1.

The simulation results agree well with experimental data for the transmitted and reflected signals and demonstrate rejection of frequencies outside the required frequency cutoff. The resonant frequency is 7.2 GHz and the bandwidth of the stopband is 0.5 GHz (7.1-7.6 GHz) with the reference level of $|S_{21}| = -10$ dB. A deep rejection band ($S_{21} > -50$ dB) is obtained at the resonant frequency with a steep cutoff; a flat passband ($S_{21} < 1.2$ dB) is observed, suggesting the proposed spiral filter design has low insertion losses thus limiting its effect on transmitted signal when integrated into a circuit.

The data can also be visualized by the electric field distribution below and at the resonant frequency. (see Figure 4) Below the resonant frequency a high level of signal is transmitted through the device; at the resonant frequency of 7.2 GHz a high level of signal is attenuated, thus demonstrating the degree of signal selectivity developed by the filter design.

Fractal Spiral Resonator Band-Stop Filter

A fractal spiral resonator developed by Palandöken & Henke is shown in Figure 5.

The filter is composed of two unit cells of electrically small artificial magnetic metamaterials formed with the direct connection of two concentric Hilbert fractal curves. Operation is based on the excitation of two electrically coupled fractal spiral resonators through direct connection with

the feeding line. Simulation results for the transmission (S_{21}) and reflection (S_{11}) losses are shown in Figure 6; the selectivity of the filter is 100 dB/GHz with a 3 dB reference insertion loss.

The electric field distribution developed by the fractal spiral resonator is shown in Figure 7; below the resonant frequency, signal passes through the filter; at resonance the signal is highly attenuated with an extremely low level of signal transmitted.

Conclusions

The performance of a spiral resonator filter has been analyzed using COMSOL Multiphysics and shown to demonstrate agreement with experimental data. A compact microstrip based spiral resonator filter with a resonant frequency of 7.2 GHz shows low insertion losses with a high level of performance and sharp cutoff over the specified frequency range. Analysis of a fractal spiral resonator consisting of two unit cells of magnetic metamaterials operating at a resonant frequency of ~1.3 GHz also shows a high level of selectivity at 100 dB/GHz. Analyses of this type can be extended to assess the performance of other filter designs prior to fabrication and integration into operating circuits. ■

REFERENCES

Ho Lim, Jong-Hyuk Lee, Sang-Ho Lim, Dong-Hoon Shin, and Noh-Hoon Myung, Proceedings of Asia-Pacific Microwave Conference 2007.

M. Palandöken, H. Henke, "Applied Electromagnetics Conference", p. 1-4, 2009.

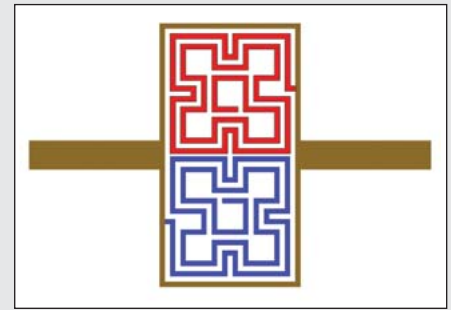


FIGURE 5: Geometry of metamaterials fractal spiral resonator: two fractal resonators are connected anti-symmetrically along the feeding line.

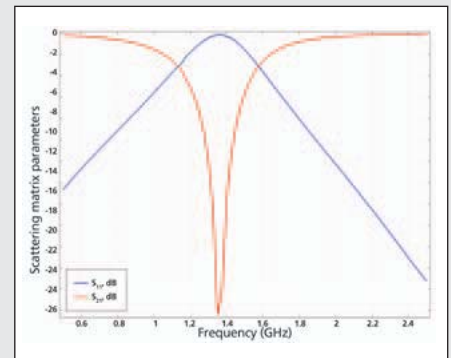


FIGURE 6: Reflection and transmission parameters of the fractal spiral resonator.

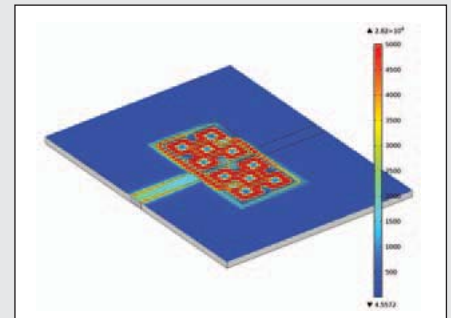
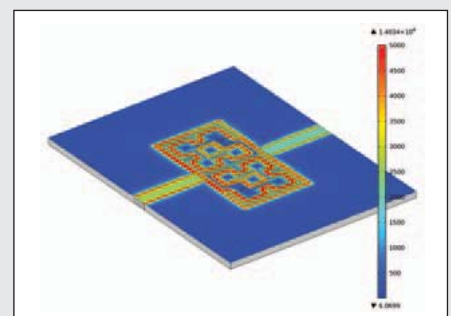


FIGURE 7: Electric field at a frequency below the resonant frequency (top) and at the resonant frequency (bottom).



The team at AltaSim Technologies.